Response to the reviewer 2

We are grateful to the referees for their time and energy in providing helpful comments and guidance that have improved the manuscript. In this document, we describe how we have addressed the reviewer's comments. Referee comments are shown in black and author responses are shown in blue text.

This study represents a new biosphere-chemistry modeling framework that simulates online, two-way interactions between surface ozone and vegetation, mainly through the linkages between stomatal conductance, leaf area index (LAI) and dry deposition. Global model-observation comparison for simulated gross primary productivity (GPP), LAI, ozone concentrations and dry deposition velocities have been conducted using a large ensemble of datasets. This work is important in laying a foundation for more indepth future studies of biosphere-atmosphere interactions. However, as of the current form the manuscript lacks enough details regarding model implementation, which I believe is important for a GMD paper. I would recommend the publication of this manuscript should the following model details are included, addressed and discussed.

➔ Thank you for your positive evaluations. All the questions and concerns have been carefully answered and the paper has been revised accordingly.

Specific comments:

P6 L129: I think here and elsewhere, the units for all variables should be included in all the equations listed.

Response: Units for all equation variables have been added in the revised paper. For Equation (1), we described it as follows: "… where r_s is the leaf stomatal resistance ($s\ m^{-1}$); m is the empirical slope of the Ball-Berry stomatal conductance equation and is affected by water stress; c_s is the CO_2 concentration at the leaf surface ($\mu mol\ m^{-3}$); RH is the relative humidity of atmosphere; b ($m\ s^{-1}$) represents the minimum leaf stomatal conductance when net leaf photosynthesis (A_{net}, $\mu mol\ m^{-2}\ s^{-1}$) is 0." (Lines 147-151)

P7 L137: Carbon allocation and LAI simulations are a very important part of the modeling framework, but no details have been given. The schemes/algorithms used for simulating carbon allocation and LAI should be described.

Response: In the revised paper, we added following descriptions in section 2.1 "Descriptions of the YIBs model" to clarify (Lines 165-184):

The YIBs model applies the LAI and carbon allocation schemes from the TRIFFID model (Clark et al., 2011; Cox, 2001). On the daily scale, canopy LAI is calculated as follows:

$$LAI = f \times LAI_{max} \tag{3}$$

Where f represents phenological factor controlled by meteorological variables (e.g., temperature, water availability, and photoperiod); LAI_{max} represents the available maximum LAI related to tree height, which is dependent on the vegetation carbon content (C_{veg}). The C_{veg} is calculated as follows:

$$C_{veg} = C_l + C_r + C_w \tag{4}$$

where C_l, C_r and C_w represent leaf, root, and stem carbon contents, respectively. And all carbon components are parameterized as the function of LAI_{max}:

$$\begin{cases} C_l = \alpha \times LAI \\ C_r = \alpha \times LAI_{max} \\ C_r = \beta \times LAI_{max}^{\gamma} \end{cases} \tag{5}$$

where α represents the specific leaf carbon density; β and γ represent allometric parameters. The vegetation carbon content C_{veg} is updated every 10 days:

$$\frac{dC_{veg}}{dt} = (1 - \tau) \times NPP - \varphi \tag{6}$$

where τ and φ represent partitioning parameter and litter fall rate, respectively, and their calculation methods have been documented in Yue and Unger (2015). Net primary productivity (*NPP*) is calculated as the residue of subtracting autotrophic respiration (R_a) from GPP:

$$NPP = GPP - R_a \tag{7}$$

P8 L157: Why is aerodynamic resistance not included in the calculation of ozone fluxes? The ozone simulated by any chemical transport model should be at the lowest model layer, but that should be different enough from the ozone concentration at the canopy top. Please justify. Moreover, shouldn't the ozone flux calculated here for ozone damage be consistent with the dry deposition velocity/flux calculation in GC? The internally inconsistent ways to represent ozone fluxes between GC and YIBs seem to reduce the usefulness of GC-YIBs as a coupling tool.

Response: Thank you for the constructive comments.

(i) The GEOS-Chem model calculates concentrations of air components at 47 vertical layers from 1013.25 to 0.01 hPa. We use [O_3] at the lowest layer to approximate O_3 concentration at the canopy top. We acknowledge the limit of this approximation in the discussion section: "(3) [O_3] at the lowest model level is used as an approximation of canopy [O_3]. The current model does not include a sub-grid parameterization of pollution transport within canopy, leading to biases in estimating O_3 vegetation damage and the consequent feedback. However, development of such parameterization is limited by the availability of simultaneous measurements of microclimate and air pollutants." (Lines 506-510)

(ii) In the original YIBs model, O_3 stomatal flux is calculated as the function of boundary layer resistance, stomatal resistance, and ambient O_3 concentration. In order to fully link GEOS-Chem with YIBs, we have updated the stomatal O_3 flux scheme to include aerodynamic resistance (which is now consistent with GEOS-Chem). At each integration step, GEOS-Chem provides both hourly aerodynamic resistance (r_a) and boundary resistance (r_b) for stomatal O_3 flux scheme in YIBs.

In the revised paper, Eq.9 $F_{O_3} = \frac{[O_3]}{r_b+k\cdot r_s}$ has been updated as $F_{O_3} = \frac{[O_3]}{r_a+r_b+k\cdot r_s}$ to take into effects of both r_a and r_b. We clarify in the revised paper as follows: "In the online GC-YIBs configuration, GC provides the hourly meteorology, <u>aerodynamic resistance, boundary layer resistance</u>, and surface [O_3] to YIBs." (Lines 259-261). Accordingly, the assessment of global O_3 damage to vegetation (section 3.3) has been updated. Compared to the original stomatal O_3 flux scheme within YIBs, the new scheme increases O_3 stomatal flux in Amazon but decreases O_3 stomatal flux in eastern China (Fig.R1c). As a result, O_3 damage on GPP decreases in eastern China but increases in Amazon (Fig.R1f).

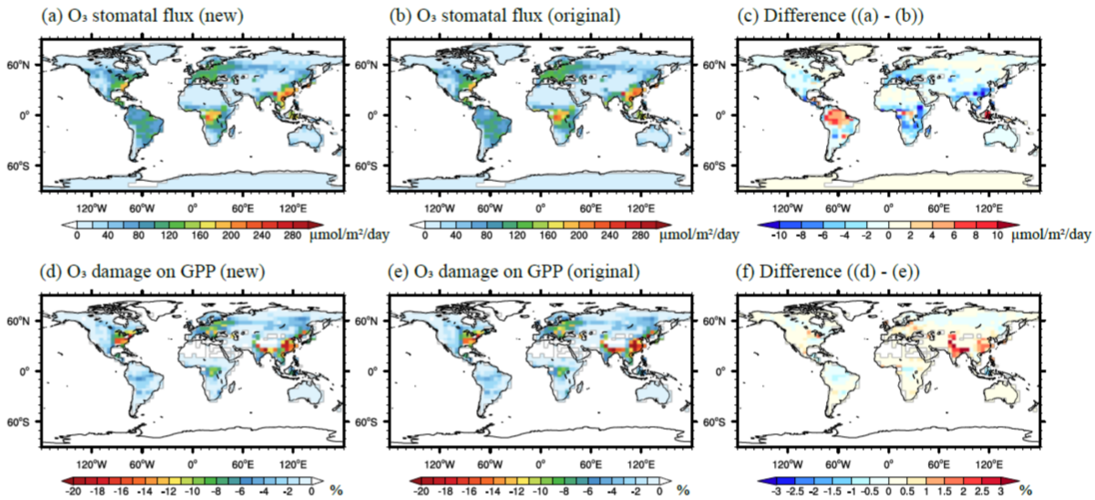

Figure R1 Comparison of O_3 stomatal flux schemes. **(a)** and **(b)** represent the O_3 stomatal flux for new and original schemes, respectively. **(c)** represents the O_3 stomatal flux difference between new and original schemes (a-b). **(d)** and **(e)** represent the O_3 damages to GPP for new and original schemes, respectively. **(f)** represents the O_3 damages difference between new and original schemes (d-e).

P8 L168: 4°×5° appears to be a rather low resolution. While the issue of computational expense is understandable, I recommend the authors to discuss how such a low resolution of simulations may interfere with the accuracy of simulated variables (ozone concentrations, GPP, etc.) as compared with observations.

Response: We run relatively high resolution (2°×2.5°) of GC-YIBs from 2006 to 2007 to have a check. The result of 2007 is used to compare the differences induced by resolutions. The following information has been added in the last part:

"The low resolution will affect local emissions (e.g., NO_x and VOC) and transport, leading to changes in surface [O_3] in GEOS-Chem. The comparison results of 2007 show that low resolution of 4°×5° induces a global mean bias of -0.24 ppbv on surface [O_3] compared to the relatively high resolution at 2°×2.5° (Fig. S7). Compared with surface [O_3], low resolution causes limited differences in vegetation variables (e.g., GPP and LAI, not shown)." (Lines 515-521).

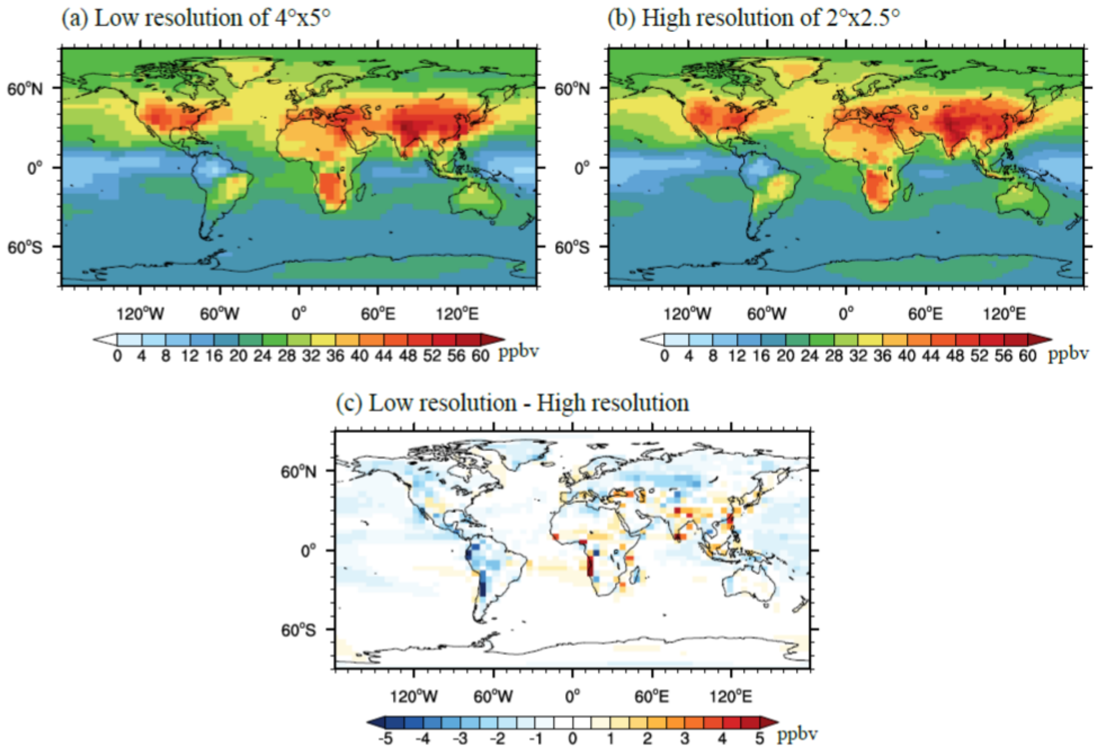

Figure S7 Comparison of MDA8 [O_3] simulated with (a) low (4°×5°) and (b) relatively high (2°×2.5°) horizontal resolutions. (c) represents the MDA8 [O_3] difference between low and high resolutions (a-b).

P10 L210: While the replacement of Olson land-type stomatal resistance with YIBs plant-functional-type (PFT) stomatal resistance is mentioned, could the authors also explain how the conversion of other land-type resistances to YIBs PFT resistances was done? In general, it would be highly useful to explain how Olson land types are matched and mapped with YIBs PFTs. A conversion table in the supplement would really help.

Response: We added Table S2 and Fig. S3 to clarify. In GEOS-Chem, the Olson land-type database are used in the calculation for dry deposition velocity. Each of the Olson land types is assigned a corresponding "deposition land type" with characteristic values of surface resistance components. There are 74 Olson land-types but only 11 deposition land-types (Table R1, i.e., many of the Olson land types share the same deposition characteristics). “The conversion relationships between YIBs land types and GC deposition land types are summarized in Table S2. The global spatial pattern of deposition land types converted from YIBs land types is shown in

Fig. S2. The Olson 2001 land cover map used in GC version 12.0.0 has a native resolution of 0.25°×0.25° and 74 land types (Olson et al., 2001). Each of the Olson land types is associated with a corresponding deposition land type with prescribed parameters. There are 74 Olson land types but only 11 deposition land types, suggesting that many of the Olson land types share the same deposition parameters. At specific grids (4°×5° or 2°×2.5°), dry deposition velocity is calculated as the weighted sum of native resolution (0.25°×0.25°). Replacing of Olson with YIBs land types induces global mean difference of -0.59 ppbv on surface [O_3] (Fig. S3). Large discrepancies are found in Africa and southern Amazon, where the local [O_3] decreases by more than 2 ppbv with the new land types. However, limited differences are shown in mid-high latitudes of Northern Hemisphere (NH, Fig. S3).” (Lines 274-287)

Table R1 The corresponding parameters for 11 deposition land types used in GEOS-Chem (http://wiki.seas.harvard.edu/geos-chem/index.php/Dry_deposition).

DD type	Description	IRI [s m^{-1}]	IRLU [s m^{-1}]	IRAC [s m^{-1}]	IRGSS [s m^{-1}]	IRGSO [s m^{-1}]	IRCLS [s m^{-1}]	IRCLO [s m^{-1}]	IVSMAX [10^{-2} cm s^{-1}]	Reference
1	Snow/Ice	9999	9999	0	100	3500	9999	1000	100	Wesely, AE, 1989
2	Deciduous forest	200	9000	2000	500	200	2000	1000	100	Wesely, AE, 1989
3	Coniferous forest	400	9000	2000	500	200	2000	1000	100	Wesely, AE, 1989
4	Agricultural land	200	9000	200	150	150	2000	1000	100	Wesely, AE, 1989
5	Shrub/grassland	200	9000	100	350	200	2000	1000	100	Wesely, AE, 1989
6	Amazon forest	200	1000	2000	200	200	9999	9999	100	Jacob & Wofsy, JGR 1990
7	Tundra	200	4000	0	340	340	9999	9999	100	Jacob et al., JGR 1992
8	Desert	9999	9999	0	1000	400	9999	9999	10	Wesely, AE, 1989
9	Wetland	200	9000	300	0	1000	2500	1000	100	Wesely, AE, 1989
10	Urban	9999	9999	100	400	300	9999	9999	100	Wesely, AE, 1989
11	Water	9999	9999	0	0	2000	9999	9999	10	Wesely, AE, 1989

Table S2. The conversion relationships between YIBs and GEOS-Chem deposition land types.

YIBs land types	GEOS-Chem deposition land types
Evergreen broadleaf forest	Amazon forest
Evergreen needleleaf forest	Coniferous forest
Deciduous broadleaf forest	Deciduous forest
Shrub land	Shrub/grassland

Tundra	Shrub/grassland
C_4 grasses	Shrub/grassland
C_3 grasses	Shrub/grassland
C_3 crops	Agricultural land
C_4 crops	Agricultural land

P11 L223: YIBs simulates stomatal conductance first at the leaf level, while GC takes in conductance at the canopy level. Appropriate scaling between the two levels should be included and discussed.

Response: In the revised paper, we clarify as follows: "The YIBs model applies Farquhar et al. (1980) scheme to calculate leaf level photosynthesis, which is further upscaled to canopy level by the separation of sunlit and shaded leaves (Spitters, 1986). The canopy is divided into an adaptive number of layers (typically 2-16) for light stratification. Sunlight is attenuated and becomes more diffusive when penetrating the canopy. The sunlit leaves can receive both direct and diffuse radiation, while the shading leaves receive only diffuse radiation. The leaf-level photosynthesis, calculated as the sum of sunlit and shading leaves, is then integrated over all canopy layers to derive the GPP of ecosystems." (Lines 125-133)

P12 L250: Four years of spin-up for LAI simulations is probably insufficient. LAI typically takes decades to stabilize, depending on the initial conditions of LAI. The authors are recommended to explain in greater detail such an issue, show whether LAI has reached a steady state in four years, and state specifically what LAI is used as the initial conditions.

Response: In the GC-YIBs model, the initial soil carbon pool and tree height are provided by the 140-year spin up procedure using offline YIBs. An earlier study (Yue and Unger, 2015) has shown that vegetation variables reached a steady state through 140 years spin up processes. In the "Descriptions of the YIBs model" section, we added: "The initial soil carbon pool and tree height used in YIBs are from the 140 years spin-up processes (Yue and Unger, 2015)". (Lines 138-140)

P14 L306: I think the authors meant Online_GS here instead of Online_LAI.

P15 L308: I think the authors meant Online_LAI here instead of Online_GS.

Response: The simulation names mentioned above are correct. 'Online_LAI' includes online LAI but offline gs, and 'Online_GS' includes online gs but offline LAI. As a result, (Online_ALL – Online_LAI) represents the changes cause by differences in gs (online vs. offline). Meanwhile, (Online_ALL – Online_GS) represents the changes caused by differences in LAI (online vs. offline).

P15 L324: The authors need to justify why BVOC changes resulting from LAI changes are not the dominant factor (in addition to stating the broadly consistent spatial patterns). How BVOC changes should influence the results and interpretation should be discussed in greater detail.

Response: The isoprene and NO_x emissions changes caused by coupled LAI has been added as Fig. S5 in the revised paper. "In a comparison, updated LAI induces limited changes in the isoprene and NO_x emissions (Fig. S5), suggesting that changes of dry deposition velocity are the dominant drivers of O_3 changes". (Lines 379-382) In Fig. 4d, $\Delta[O_3]$ induced by updated LAI show limited changes globally (by 0.05 ppbv) and moderate changes in tropical regions. Such changes mainly because the LAI predicted by YIBs is close to MODIS LAI used in GC (Fig.2).

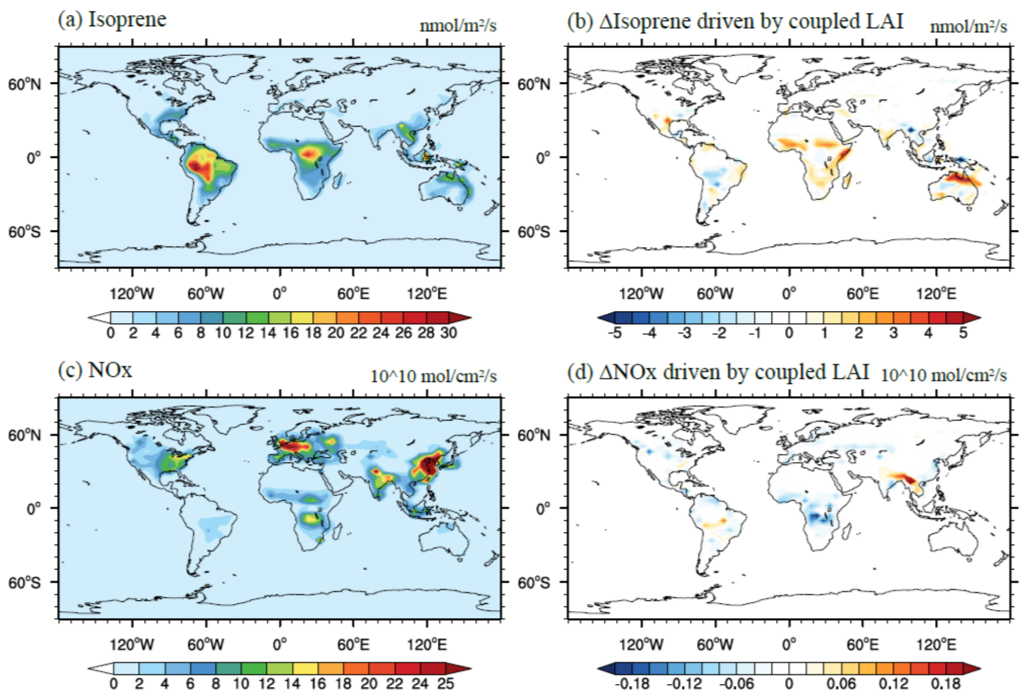

Figure S5 Simulated annual isoprene (a) and NO_x (c) emissions from online GC-YIBs model and its changes (b-d) caused by coupled LAI averaged for period of 2010-2012.

References

Clark, D., Mercado, L., Sitch, S., Jones, C., Gedney, N., Best, M., Pryor, M., Rooney, G., Essery, R., and Blyth, E.: The Joint UK Land Environment Simulator (JULES), model description–Part 2: carbon fluxes and vegetation dynamics, Geoscientific Model Development, 4, 701-722, 2011.

Cox, P. M.: Description of the" TRIFFID" dynamic global vegetation model, 2001. 2001.

Farquhar, G. D., Caemmerer, S. V., and Berry, J. A.: A Biochemical-Model of Photosynthetic Co2 Assimilation in Leaves of C-3 Species, Planta, 149, 78-90, 1980.

Olson, D. M., Dinerstein, E., Wikramanayake, E. D., Burgess, N. D., Powell, G. V. N., Underwood, E. C., D'Amico, J. A., Itoua, I., Strand, H. E., Morrison, J. C., Loucks, C. J., Allnutt, T. F., Ricketts, T. H., Kura, Y., Lamoreux, J. F., Wettengel, W. W., Hedao, P., and Kassem, K. R.: Terrestrial ecoregions of the worlds: A new map of life on Earth, Bioscience, 51, 933-938, 2001.

Spitters, C.: Separating the diffuse and direct component of global radiation and its implications for modeling canopy photosynthesis Part II. Calculation of canopy photosynthesis, Agr Forest Meteorol, 38, 231-242, 1986.

Yue, X. and Unger, N.: The Yale Interactive terrestrial Biosphere model version 1.0: description, evaluation and implementation into NASA GISS ModelE2, Geoscientific Model Development, 8, 2399-2417, 2015.